

Phosphorous modified ZSM-5: Deactivation and product distribution for MTO

Mads Kaarsholm^a, Finn Joensen^b, Jesper Nerlov^b, Roberta Cenni^b, Jamal Chaouki^a,
 Gregory S. Patience^{a,*}

^aDepartment of Chemical Engineering, École Polytechnique de Montréal, Canada

^bHaldor Topsøe A/S, Denmark

Received 17 June 2006; received in revised form 14 December 2006; accepted 27 December 2006
 Available online 16 January 2007

Abstract

The product distribution and deactivation in the methanol-to-olefin (MTO) process over a phosphorous modified catalyst containing 10% H-ZSM-5 was studied in small diameter fixed bed reactors. These studies suggest that methane is formed directly from methanol and/or dimethyl ether and that non-aromatic C₅₊ hydrocarbons are intermediates in the MTO reaction, forming light olefins (C₃= and C₄=, but *not* ethylene) by secondary cracking reactions. Based on photographs of the catalyst taken during the course of the reaction, three distinct coking patterns were observed that might be attributable to the different reactions. Deactivation time of the catalyst is highly dependent on the contact time, doubling the feed rate decreased the deactivation time by a factor of 10 and lowered the olefin production. Changing the feed from pure methanol to 10% methanol in nitrogen reduced methanol capacity of the catalyst considerably, but a slight increase in propylene selectivity was also observed.

© 2007 Elsevier Ltd. All rights reserved.

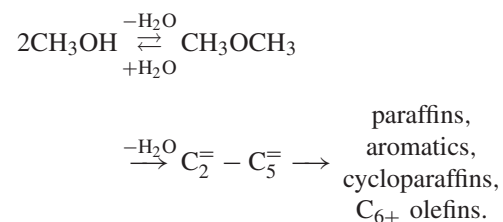
Keywords: Catalyst deactivation; Zeolites; Catalyst selectivity; ZSM-5; Methanol-to-olefins

1. Introduction

The methanol to hydrocarbon process over acid zeolites has received significant academic and industrial attention since its discovery in the late 1970s (Chang, 1984). In the last two decades the main focus of this research has been on the methanol-to-olefin (MTO) part of the reaction due to the increasing demand for light olefins (Chen et al., 2005). This has become even more pronounced with the high price of crude oil. The MTO process is an acid catalyzed reaction of which SAPO-34 and ZSM-5 are the most common catalysts (Stöcker, 1999).

Several kinetics/reaction paths have been proposed for the MTO and MTG process. Chang and Silvestri (1977) proposed

the first model.



Equilibrium between MeOH and DME is reached very rapidly. This mixture then reacts to form light olefins followed by paraffins and aromatics. In early kinetic studies, the two oxygenates were treated as a single species (Chang, 1983; Keil, 1999). In addition, the kinetic rates were derived for fresh catalyst and deactivation was ignored. Aguayo et al. (2005) modelled the reaction kinetics and deactivation for both ZSM-5 and SAPO-18 catalysts and accounted for both the deactivation due to coking and irreversible activity loss that occurs with each regeneration cycle. However, their model lumped the light olefins into

* Corresponding author. Tel.: +1 514 340 4711x3439.

E-mail address: gregory-s.patience@polymtl.ca (G.S. Patience).

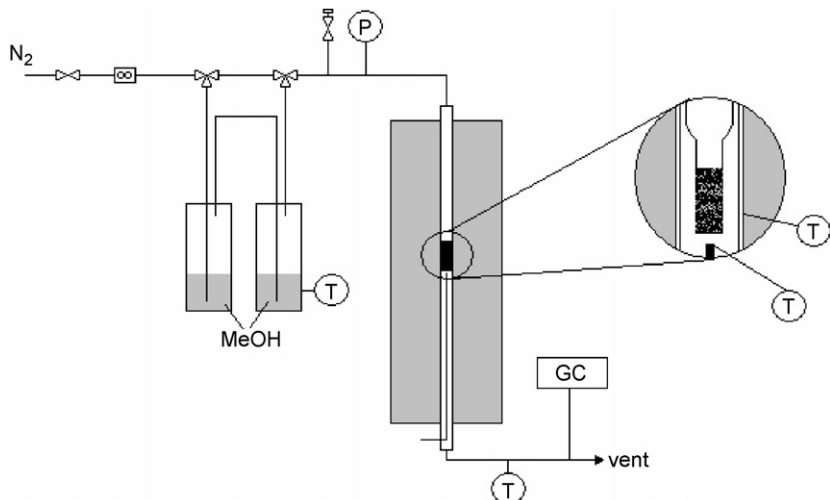


Fig. 1. Experimental setup.

one component and is therefore unsuitable for differentiating between ethylene and propylene yield.

Detailed models have been proposed by Mihail et al. (1983) and Park and Froment (2001a,b) who characterized the process based on elementary reactions. Mihail et al. (1983) considered 27 reactions for the C1–C5 fractions and an additional 26 for higher hydrocarbons. Dehertog and Froment (1991) examined the effect of phosphorus on H-ZSM-5 catalysts. They showed that the space velocity had to be reduced by 75% in order to achieve the same conversion compared to the non-modified zeolite. The phosphorous modification increased the lower olefin yield at low temperature; at high temperature (480 °C), the effect of phosphorus was not as pronounced. Other investigations of P-modified ZSM-5 showed a similar decrease in conversion and increase in selectivity of up to 70% at complete methanol conversion (Froment et al., 1992).

Chen et al. (2000) investigated the effect of space velocity over a SAPO-34 catalyst. They found that the coking rate was lower with high methanol feed rates under partial methanol conversion conditions. This was also observed for ZSM-5 by Benito et al. (1996). The increased coking rate was largely attributed to the increased conversion of oxygenates and, to a small extent, to the space velocity. Chen et al. (2000) found that the coke content was proportional to the amount of hydrocarbon formed (per mass of catalyst) and independent of space velocity.

In the present study, the effect of space velocity, temperature and reactor diameter on the activity profile of the catalyst is reported. These parameters are important in the design of MTO reactors for both fixed and fluid bed processes.

2. Experimental

2.1. Catalyst

The catalyst was made of 10% CBV28014 (from Zeolyst) imbedded in an Si/Al matrix consisting of Catapal B, Levasil 100s/30% and kaoline which was spray dried and calcined in air at 550 °C for 4 h. The average particle size of the

resulting catalyst was 100 µm. The powder was contacted with an (NH₃)₂HPO₄ solution and then dried and calcined so that the resulting catalyst contained 1.5% phosphorus. It was made into tablets, crushed and sieved into a fraction of 400–600 µm.

2.2. Reactor setup

The experimental setup is shown in Fig. 1. The experiments were conducted in an 8 mm stainless steel reactor and a 9 mm inner diameter quartz reactor into which a 3 or 6 mm inner diameter quartz tube could be inserted. The outer diameters of the two insertion tubes were 5.0 and 8.0 mm resulting in an annulus between the inner and outer tubes of 2 and 0.5 mm, respectively. The small insertion tube expanded to an outer diameter of 8.2 mm approximately 3 cm above the catalytic bed reducing the length of the larger annulus to a minimum. The vessel was heated electrically and the temperature was regulated with a PID controller. The distance between the 9 mm quartz tube and the heater was 1.75 mm. The reference temperature for control was measured at the wall of the heater. The temperature at the reactor exit was monitored by a thermocouple placed in a thermowell 10 mm below the bed. Additional thermocouples were inserted in the catalyst bed. When the feed gas was switched from nitrogen to a 10% methanol in nitrogen mixture, the bed temperature rose 3 °C. The pressure in the reactor was maintained between 0 and 0.1 barg for all experiments.

The feed stream was prepared by passing nitrogen through two saturation evaporators containing MeOH: the first was kept at room temperature and the second at 16 °C to maintain a 9:1 nitrogen to methanol ratio. A Brooks 5850TR flow controller was used for the nitrogen feed gas. The product stream was analyzed by FID on a Hewlett Packard 5890 series-II GC equipped with a pre-column (Porapak Q 80/100 mesh size—0.5 m × 2.16 mm ID × 1/8 in OD packed column in stainless steel) followed by a capillary column: CP-PoraPLOT Al₂O₃, KCl—10 m × 530 µm × 5 µm. A GC with a TCD measured the CO/CO₂ and other light gases for some experiments.

2.3. Procedure

The 3 and 6 mm ID reactors were loaded with 0.185 and 0.53 g, respectively, to obtain equal bed lengths. Experiments with 100% MeOH were conducted in the 8 mm reactor with 1 g of catalyst. The reactor was heated to a given set-point in nitrogen before feeding reaction gases. The flow rate was varied between WHSV 0.22 and 2.4 h⁻¹ (based on total catalyst mass). Product gases were analyzed on-line and the experiments were terminated when equilibrium mixtures of MeOH and DME were detected.

3. Results

The experiments showed that the space velocity had a significant influence on the deactivation rate and product distribution. Fig. 2 shows the product distribution at two space velocities and

500 °C in the 6 mm reactor. The carbon mass balance was based on C₁–C₉ hydrocarbons only. Production of higher hydrocarbons, CO and CO₂ in the product gas and carbon deposition on the catalyst were neglected. The figure shows that the deactivation rate depends on the methanol feed rate: methanol breakthrough occurred after 40 h at a WHSV of 0.22 h⁻¹ (Fig. 2a) compared to less than 5 h at a WHSV of 0.43 h⁻¹ (Fig. 2b). By increasing the WHSV to 0.86 h⁻¹, the C₅₊ fraction increased and methanol breakthrough was observed after only a few minutes. The experiments show that the olefin yield decreases with increasing flow rate, which is contrary to some experiments reported in the literature over pure zeolite (Park and Froment, 2001b; Dessau, 1986).

The product distribution of the experiments conducted in the 3 and 6 mm reactors after 2 h on stream is given in Table 1. As expected both the yield of light olefins and methane increase with temperatures. However, at 500 °C and partial methanol conversion, increased space velocities resulted in a decrease in olefin selectivity. At the highest space velocity (WHSV of 1.43 h⁻¹) in the 3 mm reactor, methane became the dominant hydrocarbon product, accounting for almost half of the total.

The first six experiments reported span the regime of partial to essentially full MeOH/DME conversion. The fact that methane predominated at the highest space velocity, where only 15% of MeOH/DME was converted into hydrocarbons, leads us to propose that methane forms in parallel to the equilibrium reaction from either MeOH or DME or from both.

At 50–70% MeOH/DME conversion, the C₅₊ fraction predominates, whereas at close to full conversion propylene was the most abundant hydrocarbon. In Fig. 3, the product distributions shown in Table 1 (500 °C data) are plotted against the MeOH/DME conversion. The plot demonstrates that: (1) methane is formed very early in the reaction, before the higher hydrocarbons; (2) at higher conversion, methane levels are largely constant and (3) as reaction progresses, the C₅₊ yield reaches a maximum and subsequently declines while the formation of light olefins accelerates. The latter observation may be rationalized in terms of higher aliphatic (and possibly naphthenic) hydrocarbons undergoing secondary cracking reactions, thus increasing the amount of light products. The data in Table 1 show that the C₅₊ fraction at low conversion is low in aromatics and, therefore, relatively labile with respect to secondary cleavage reactions. The sequence of reactions described above may also explain both the coking pattern (vide infra) and the fact that, in experiments conducted at low space velocity with complete MeOH/DME conversion, C₅₊ yields tend to increase as breakthrough approaches. This peak in C₅₊ yields at close to full conversion is apparent from Fig. 2a and b. It is also evident from Fig. 4, showing the product distribution as a function of MeOH/DME conversion in an integral experiment conducted with a feed of 100% methanol. Fig. 4 also shows that the ethylene yield closely parallels that of the aromatics (predominantly xylenes and trimethylbenzenes). This trend agrees with recent data published by Svelle et al. (2006) who concluded that ethylene is formed from xylene and trimethylbenzene intermediates rather than from secondary alkene cracking reactions. Also apparent from Fig. 4 is the fact

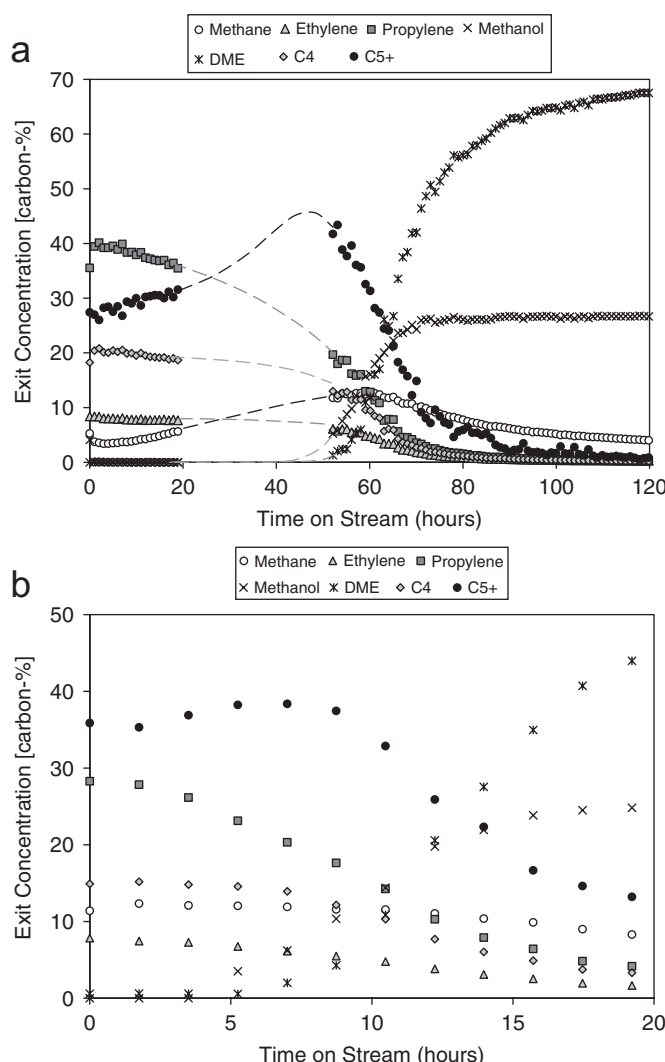


Fig. 2. MTO product distribution at 500 °C in the 6 mm inner diameter reactor with 10% methanol in nitrogen feed: (a) WHSV 0.22 h⁻¹ (dashed lines due to missing data), (b) WHSV 0.43 h⁻¹.

Table 1

Product distribution after 2 h on stream in the 3 and 6 mm diameter reactors

Reactor diameter (mm)	3	3	3	6	6	6	6	6
Temperature	500	500	500	500	500	500	450	400
WHSV (h^{-1})	1.47	0.87	0.43	0.86	0.43	0.22	0.23	0.25
Contact time (s)	0.18	0.31	0.63	0.32	0.63	1.25	1.24	1.24
<i>Product distribution (%)</i>								
Methane	7.2	7.8	7.6	5.3	12	3.6	2	1.2
Ethane	0.3	0.3	0.4	0.2	0.8	0.2	0.1	0.1
Ethylene	0.9	3.1	7.3	2	7.5	8.3	5.4	2.7
Propane	0.1	0.1	0.6	0.1	0.4	0.9	0.6	0.1
Propylene	2	11	32	8.1	28	40	39	16
Methanol	16	22	1	14	0.6	0.1	0	17
DME	69	27	0.1	16	0	0	0.3	28
C ₄	1.5	7.8	17	6	15	21	24	11
C ₅₊	2.9	21	33	48	35	26	29	24
Sum	99.9	100.1	99	99.7	99.3	100.1	100.4	100.1
Aromatics	0.5	4.6	11.9	7.6	17	13.1	5.8	1.5
Aromatics (in C ₅₊ fraction %)	18.7	21.7	35.4	16	48.1	50.5	19.8	6.3
% MeOH/DME conversion	15	51	98.9	70	99.4	99.9	99.7	55

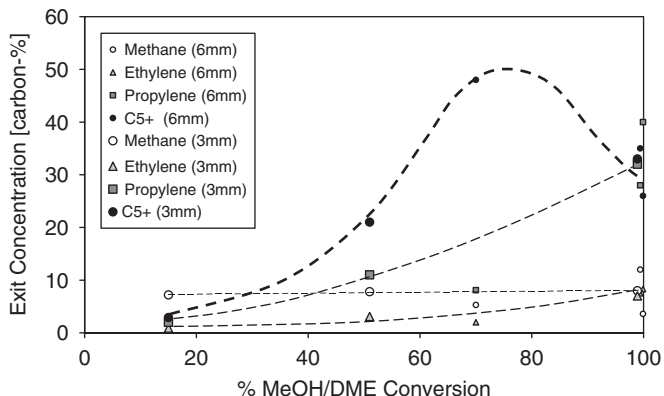
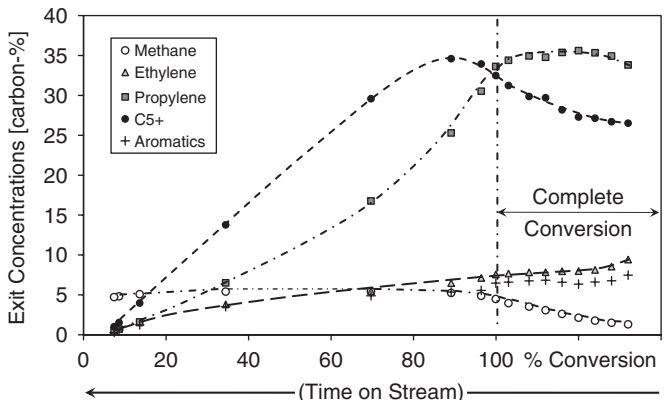


Fig. 3. Hydrocarbon distribution as a function of oxygenate conversion, based on experiments in Table 1 at 500 °C.

Fig. 4. Hydrocarbon distribution as a function of oxygenate conversion, based on experiment at 500 °C in 8 mm inner diameter reactor with pure methanol feed. WHSV 2.37 h^{-1} .

that methane formation gradually increases as breakthrough is approached and subsequently remains virtually constant. This is in full accordance with the suggestions presented above, namely that methane is formed directly from MeOH and DME:

in the early stages of the MTO reaction MeOH and DME are completely converted in a narrow zone close to the reactor entrance. As coking progresses the zone where MeOH and DME are present gradually expands through the catalyst bed and the methane formation increases. After breakthrough, i.e., when MeOH and DME extend the full catalyst bed, methane formation reaches a maximum and stays constant thereafter.

We considered channelling as a possible mechanism to account for the lower olefin production at higher flow rates. The average particle diameter to tube ratio in the 8, 6 and 3 mm inner diameter reactors was 16, 12 and 6, respectively, and these values are greater than the standard rule of thumb of 10 for the two larger reactors. In the case of the 3 mm reactor, some channelling might have occurred over a limited length of the bed. However, channelling is considered to be negligible when the bed length to tube diameter is greater than 10, which was the case of the 3 mm reactor. After unloading the catalyst from the reactor, radial gradients of color at various distances from the bed entrance were not seen. Finally, all recorded data of the exit composition showed that the MeOH/DME equilibrium was established. Thus, we conclude that channelling effects were insignificant.

In Fig. 2a breakthrough occurred after less than 50 h. In a comparative experiment using 100% MeOH as a feed and maintaining almost the same contact time (1.13 s) the time until breakthrough was 10 h. Taking into account the total methanol (100% vs. 10%) feed and reaction time (10 h vs. < 50 h), the capacity of the catalyst to react is at least twice as high when the feed is 100% MeOH. The increased methanol capacity with pure methanol may be attributable to the higher water vapor pressure that reduces the coking rate (Gayubo et al., 2004). The product distribution was slightly different with diluted methanol; notably propylene yields were higher whereas the C₄ fraction was lower at the low methanol concentration. Whereas there is virtually no difference in ethylene yields supporting the two different reaction pathways for ethylene and propylene. With pure MeOH feed, methane formation was

significantly reduced, probably due to the higher water partial pressure.

With respect to coking, nitrogen QBET measurements clearly demonstrate a reduction in pore volume of the deactivated catalyst over the entire range, as shown in Fig. 5. The total pore volume of the fresh, coked and regenerated samples were 0.207, 0.0973 and $0.202\text{ cm}^3/\text{g}$. The lower volume may be attributable to two mechanisms: accumulated surface carbon deposition and blocking of the pore entrances to the pores. The regenerated catalyst was treated with air at 500°C and, in the region of $20\text{--}1000\text{ \AA}$, its pore volume distribution is identical to that of the fresh catalyst. However, in the range of $13\text{--}20\text{ \AA}$ there appears to be a minor difference between the two. The pore volume of the coked catalyst was unexpectedly higher in this region.

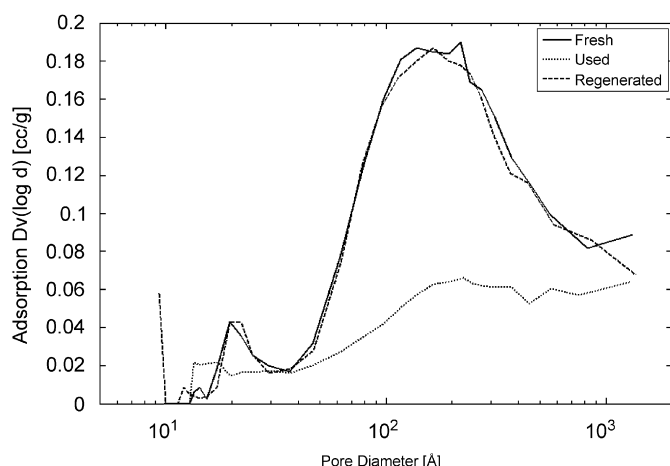


Fig. 5. Pore size distribution of fresh, coked and regenerated catalyst.

Fig. 6 demonstrates the coking pattern along the reactor: very quickly the color changes from beige to gray (less than 10 min) and three distinct regions become evident as shown in Fig. 6c: the middle of the bed is darkest gray; the entrance region (upper box) is slightly brighter and, in the exit region of the bed (lower box), there is a gradient of color from dark to light gray going down the reactor. These observations may be rationalized as follows: at the entrance, MeOH and DME reach equilibrium and C–C bond formation occurs to a limited extent. In the middle section, olefin production dominates together with methylbenzenes, the reactive intermediates of the MTO and MTG reactions (Arstad and Kolboe, 2001; Svelle et al., 2006). Chen et al. (2000) found that the oxygenate to olefin reaction was the main source of coke. In the last section, coking continues but only to a limited extent and most likely due to secondary cracking reactions as all oxygenates would have been consumed. Coking by hydrocarbon decomposition at high temperatures due to significant temperature increase from the exothermic reaction could be ruled out since temperature measurements indicated that the bed was isothermal.

The coking pattern shown in Fig. 6 is representative of the product distribution given in Fig. 2b. The product distribution was almost constant during the first 3 h corresponding to the coking pattern in Fig. 6b–f. The product distribution appears to be independent of the coke deposition. Methanol breakthrough is observed a short time after Fig. 6f, which indicates that the strong acid sites are inaccessible.

4. Conclusions

Experiments conducted at high space velocities in the regime of partial to essentially full methanol and dimethyl ether

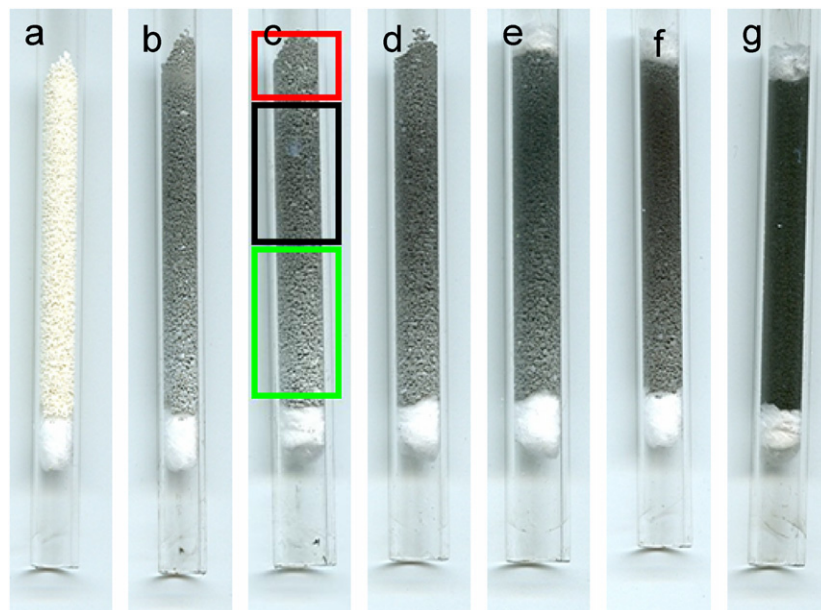


Fig. 6. Catalyst coking at $t = 0, 10, 20, 50, 110, 170, 1310\text{ min}$ in the 6 mm reactor, 10% MeOH in nitrogen, $T = 500^\circ\text{C}$, WHSV $0.43\text{ g(MeOH)/gcat/h}$ (gas flows from the top down through the bed).

conversion suggest that methane is formed directly from methanol and/or dimethyl ether. The largely non-aromatic C₅₊ intermediates predominate up until 100% MeOH/DME conversion. At this point, propylene yield is highest due to the cleavage of the C₅₊ fraction. Increasing the feed flow rate lowered the olefin production even at complete oxygenate conversion. The formation of ethylene closely parallels the aromatics, suggesting that it is by splitting off from xylene and trimethylbenzene intermediates in accordance with the labelling studies made by Svelle et al. (2006).

In the region of full oxygenate conversion, catalyst deactivation depended on contact time: doubling the feed rate (from a WHSV of 0.22 to 0.43 h⁻¹) decreased the deactivation time by a factor of 10. As a result, the methanol capacity of the catalyst increased significantly as the feed rate was reduced.

The product distribution and catalyst methanol capacity (kg of MeOH converted per kg of catalyst) are highly dependent on the feed composition. At reduced MeOH partial pressure (10% methanol in nitrogen), the olefin production was higher compared to pure methanol feed. At the same time, the methanol capacity of the catalyst was decreased significantly. Clearly, increasing the methanol partial pressure increases the catalyst methanol capacity, while increasing the methanol feed by increasing the space velocity decreases the methanol capacity. This is in contrast to the finding of Chen et al. (2000) for the SAPO-34 catalyst where they concluded that the coke deposition was based on the amount of methanol converted and temperature but not on WHSV.

Based on photographs of catalyst taken at intervals during an experiment, coking rates are low at the reactor entrance where the MeOH/DME reaches equilibrium. The main coking is due to the oxygenate to olefin and intermediates reaction. Following the main reaction zone, coking rates are low as only secondary cracking reactions occur and because the water level has reached its maximum.

References

- Aguayo, A.T., Gayubo, A.G., Vivanco, R., Alonso, A., Bilbao, J., 2005. Initiation step and reactive intermediates in the transformation of methanol into olefins over SAPO-18 catalyst. *Industrial and Engineering Chemistry Research* 44 (19), 7279–7286.
- Arstad, B., Kolboe, S., 2001. The reactivity of molecules trapped within the SAPO-34 cavities in the methanol-to-hydrocarbons reaction. *Journal of the American Chemical Society* 123, 8137–8138.
- Benito, P.L., Gayubo, A.G., Aguayo, A.T., Castilla, M., Bilbao, J., 1996. Concentration-dependent kinetic model for catalyst deactivation in the MTG process. *Industrial and Engineering Chemistry Research* 35, 81–89.
- Chang, C.D., 1983. Hydrocarbons from methanol. *Catalysis Reviews—Science and Engineering* 25, 1–118.
- Chang, C.D., 1984. Methanol conversion to light olefins. *Catalysis Reviews—Science and Engineering* 26 (3&4), 323–345.
- Chang, C.D., Silvestri, A.J., 1977. The conversion of methanol and other O compounds to hydrocarbons over zeolite catalysts. *Journal of Catalysis* 47, 249–259.
- Chen, D., Rebo, H.P., Grønvold, A., Moljord, K., Holmen, A., 2000. Methanol conversion to light olefins over SAPO-34: kinetic modeling of coke formation. *Microporous and Mesoporous Materials* 35–36, 121–135.
- Chen, J.Q., Bozzano, A., Glover, B., Fuglerud, T., Kvisle, S., 2005. Recent advancements in ethylene and propylene production using the UOP/hydro MTO process. *Catalysis Today* 106, 103–107.
- Dehertog, W.J.H., Froment, G.F., 1991. Production of light alkenes from methanol on ZSM-5 catalysis. *Applied Catalysis* 71, 153–165.
- Dessau, R.M., 1986. On the H-ZSM-5 catalyzed formation of ethylene from methanol or higher olefins. *Journal of Catalysis* 99, 111–116.
- Froment, G.F., Dehertog, W.J.H., Marchi, A.J., 1992. Zeolite catalysis in the conversion of methanol into olefins. *Catalysis* 9, 1–64.
- Gayubo, A.G., Aguayo, A.T., Atutxa, A., Prieto, R., Bilbao, J., 2004. Role of reaction-medium water on the acidity deterioration of a HZSM-5 zeolite. *Industrial and Engineering Chemistry Research* 43, 5042–5048.
- Keil, F.J., 1999. Methanol-to-hydrocarbons: process technology. *Microporous and Mesoporous Materials* 29, 49–66.
- Mihail, R., Straja, S., Maria, G., Musca, G., Pop, G., 1983. Kinetic model for methanol conversion to hydrocarbons. *Chemical Engineering Science* 38, 1581–1591.
- Park, T.-Y., Froment, G.F., 2001a. Kinetic modeling of the methanol to olefins process. 1. Model formulation. *Industrial and Engineering Chemistry Research* 40, 4172–4186.
- Park, T.-Y., Froment, G.F., 2001b. Kinetic modeling of the methanol to olefins process. 2. Experimental results, model discrimination, and parameter estimation. *Industrial and Engineering Chemistry Research* 40, 4187–4196.
- Stöcker, M., 1999. Methanol-to-hydrocarbons: catalytic materials and their behaviour. *Microporous and Mesoporous Materials* 29, 3–48.
- Svelle, S., Joensen, F., Nerlov, J., Olsbye, U., Lillerud, K.P., Kolboe, S., Bjørgen, M., 2006. Conversion of methanol to hydrocarbons over zeolite H-ZSM-5: ethylene formation is mechanistically separated from the formation of higher alkenes. *Journal of the American Chemical Society* 128 (46), 14770–14771.